Journal of Nematology 24(4):571–577. 1992.

Line Detection and Texture Analysis for Automatic Nematode Identification

J. FDEZ-VALDIVIA,[1] N. PÉREZ DE LA BLANCA,[1] P. CASTILLO,[2] AND A. GÓMEZ-BARCINA[3]

Abstract: This paper is the second in a series studying procedures for estimating and calibrating features of nematodes from digital images. Two kinds of features were analyzed for recognition: those with a directional component and those with a textural component. Features that have a directional component (lateral field and annules) were preprocessed with classic algorithms and modified by directional filters. Features having texture (esophagus and intestine) were analyzed with vectors of measures to define them and the statistical technique CART (classification and regression trees) to explain the role that each measure plays in the identification and discrimination process.

Key words: automatic identification, classification, digital image, *Dorylaimus* sp., line detection, *Mesocriconema* sp., nematode, *Rotylenchus cazorlaensis, Rotylenchus magnus,* texture, *Tylenchorhynchus* sp.

Image analysis offers techniques for objective and precise identification of the morphological features necessary for the construction of automatic methods of identification and classification. These techniques have been used in nematological investigations only recently (7). Some features of nematodes have a directional component or can be represented through textures of tissues and organs. In these cases, image analysis through filter theory (4,8) or texture analysis (5,6) makes it possible to characterize and identify such features. Classification and regression trees (CART) are very useful for texture classification (1). These methods are concerned with the use of data to form prediction rules for one measure based on the values of other measures. In classification, one makes measurements on an object and then uses some sort of prediction rule to decide what class the object is in. The algorithms presented in this paper may be used for the identification of all features in which textures or directionality are an essential component.

Received for publication 19 May 1992.

[1] Departamento de Ciencias de la Computacion e Inteligencia Artificial, Facultad de Ciencias, Universidad de Granada, 18071 Granada, Spain.

[2] Instituto de Agronomia y Proteccion Vegetal, Consejo Superior de Investigaciones Cientificas, Apartado 3048, 14080 Cordoba, Spain.

[3] Centro de Investigacion y Desarrollo Agrario, Camino de Purchil s/n, Apartado 2027, 18080 Granada, Spain.

The authors thank M. A. Gonzalez Pais for her technical assistance.

MATERIALS AND METHODS

Nematode specimens: Specimens selected for this study were collected through surveys of natural and cultivated soils in southeastern Spain, extracted from soil samples by centrifugation (3), then killed by gentle heat and fixed in 4% formaldehyde. Some specimens were processed into glycerin (9,10).

Obtaining and cleaning the image: Homogeneous images for processing were obtained as previously described (7).

Hardware and software: Images were captured (512 × 512 in size with 256 grey levels) with a system previously described (7). They were preprocessed with a SUN SPARC 2 workstation with custom-made programs written in C language. CART software (1) was used for classification.

Feature set: Cuticular features estimated were the number of lines in the lateral field, the coarseness of annules, and the textural features analyzed for the esophagus and intestine.

Mathematical background

The basic tools used for image analysis are as follows:

Filters: (See (4) for a complete explanation of the terms and concepts used below.) We express the convolution operation through scalar products, so that $\mathbf{P'X}$ (P′ transposed of P), represents the convolution of mask P (represented by a vector

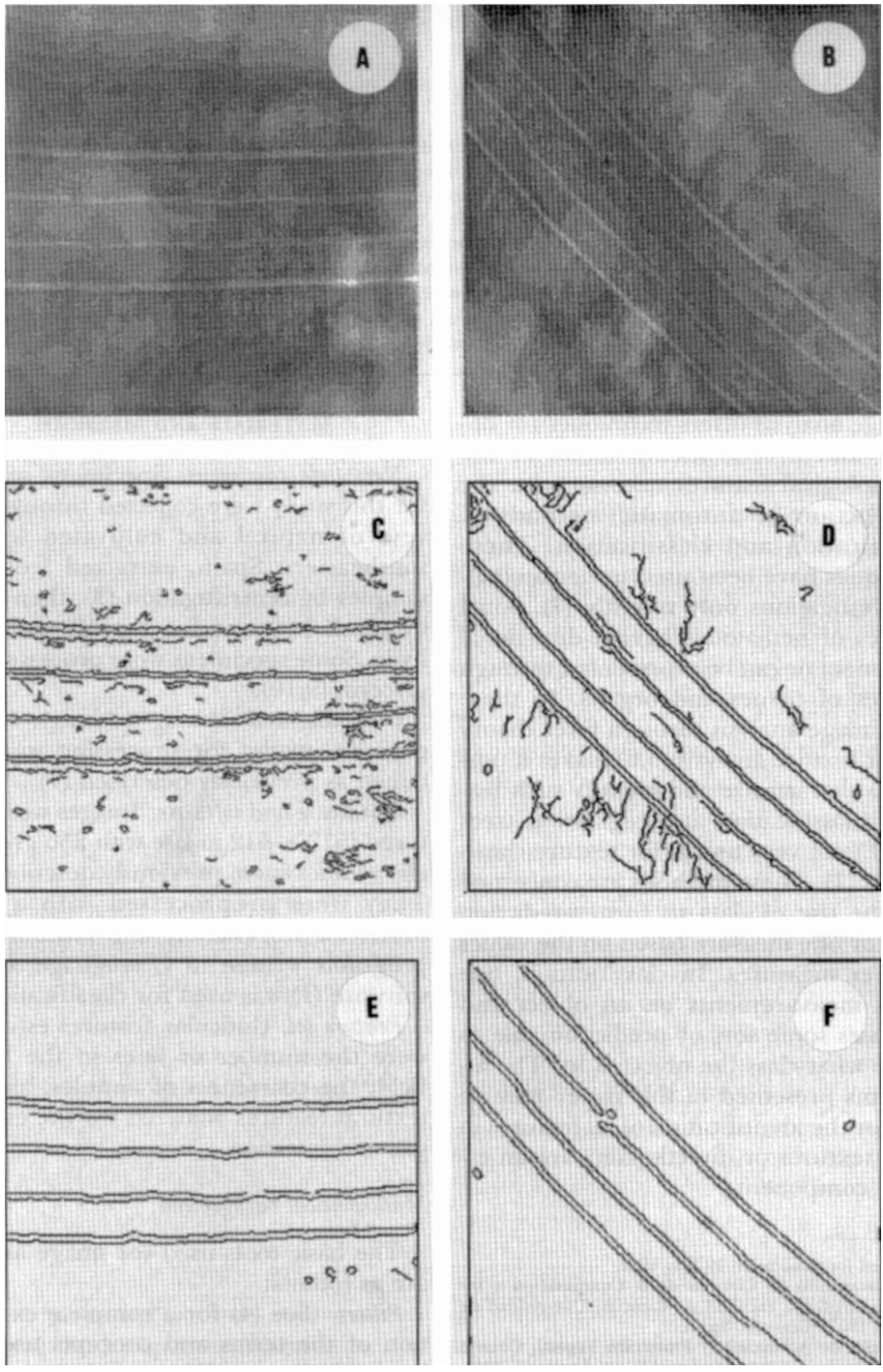

FIG. 1. A,B) Digital images of *Rotylenchus magnus* and *R. cazorlaensis* with four-line lateral fields. C,D) The results of applying the Canny filter directly to the images A–B, respectively. E,F) The results of applying the Canny algorithm on the filtered image preprocessed with a directional filter.

of values) and the portion of image X (represented by a vector as well), to which we apply the directional mask used:

Edges

$$S = (1/k)\begin{bmatrix} a & b & a \\ 0 & 0 & 0 \\ -a & -b & -a \end{bmatrix}$$

Lines

$$L = (1/k')\begin{bmatrix} -c & -c & -c \\ d & d & d \\ -c & -c & -c \end{bmatrix}$$

$$a,b,c,d > 0,\ b > a,\ c < d$$

and their corresponding rotation in the direction of the grid. Constants used (valids in all cases) were $a = c = 1$, $b = d = 2$, $k = 4$, and $k' = 18$.

With these masks the filter we apply to the image is:

$$I^*(x,y) = I(x,y) \cdot F_1(x,y) \cdot F_2(x,y)$$

with

$$F_1(x,y) = \operatorname{Max}_i\{|S_i X|\}\ F_2(x,y)$$

$$= \operatorname{Max}_i\{|L_i X|\} \qquad i = 1, \ldots, 4$$

with "*" the convolution operation, I the original image, and I* the filtered image.

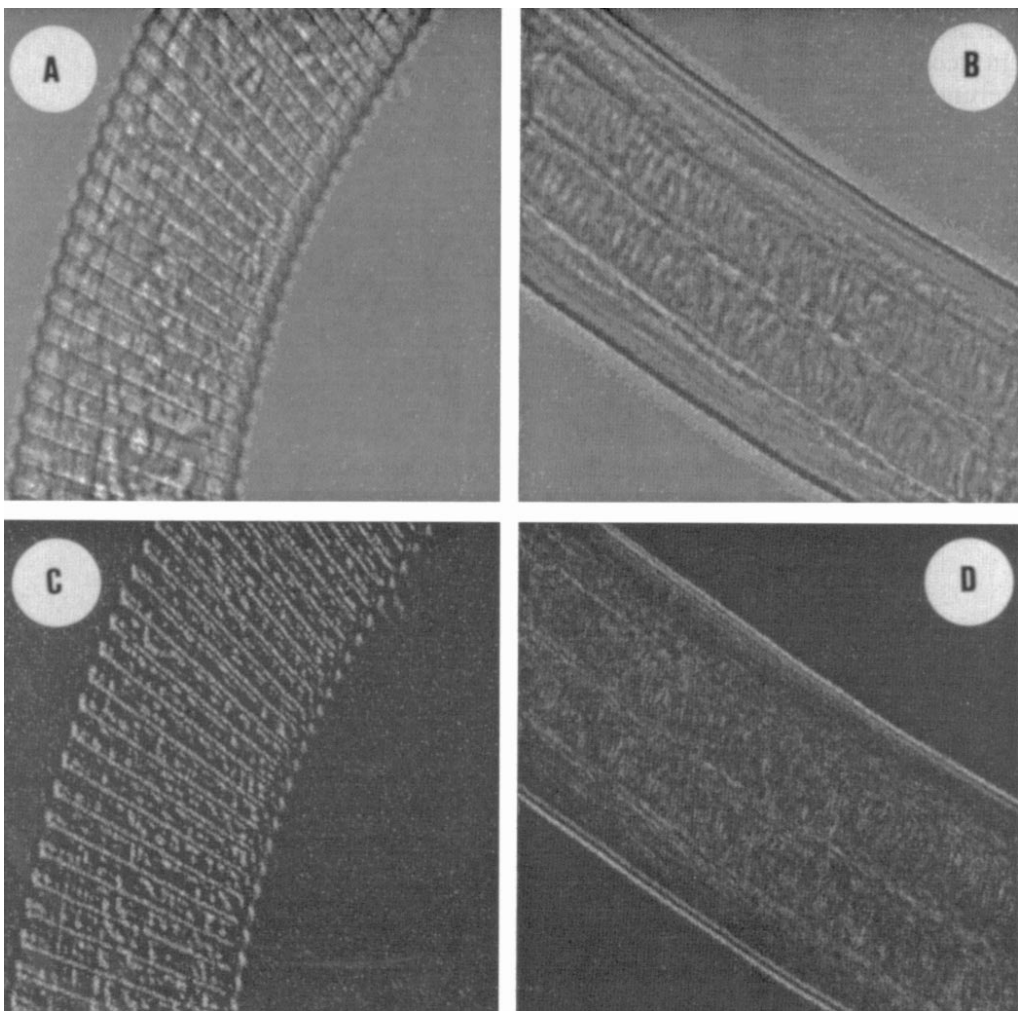

FIG. 2. A,B) Examples of two digital images of *Mesocriconema* sp. with coarse annules and *Dorylaimus* sp. without annules. C,D) The resultant images of A–B using a directional filter.

The main purpose of the filter is to determine the tendency that best fits locally each portion of the image (maximum of the cross correlation). The direction of the main edges (which we use in the recounting process) is calculated by:

$$\text{DIR}(x,y) = \arctan(|S'_1X|, |S'_2X|) \cdot 180.0/\pi \quad \text{with } a = 1,\ b = 2.$$
$$-180.0 \leq \text{DIR} \leq 180.0$$

Textures: (See (6) for details.) Different statistical measures to identify textures were used. For example, the measures based on differences of grey levels in which the 2-D histogram representing the number of occurrences in the image of each difference of grey level according to a particular vector of displacement were calculated.

We assigned $\delta = (\Delta_x,\Delta_y)$ to the displacement vector (Δ_x,Δ_y integers), D (δ) to the difference of grey levels in a distance δ: $D(\delta) = |I(i, j) - I(i + \Delta_x, j + \Delta_y)|$, and $H(d_s,\delta)$ to the probability that a particular difference d_s will occur according to the vector of displacement δ. The measures we considered from H were:

$$\mu_d = \sum_{k=1}^{n} d_k \times H(d_k,\delta) \quad \text{(measure } x_5)$$

$$C_d = \sum_{k=1}^{n} d_k^2 \times H(d_k,\delta) \quad \text{(measure } x_6)$$

$$E_d = -\sum_{k=1}^{n} H(d_k,\delta) \times log\ H(d_k,\delta) \quad \text{(measure } x_7)$$

$$A_d = \sum_{k=1}^{n} H(d_k,\delta)^2 \quad \text{(measure } x_8) \qquad \text{(A)}$$

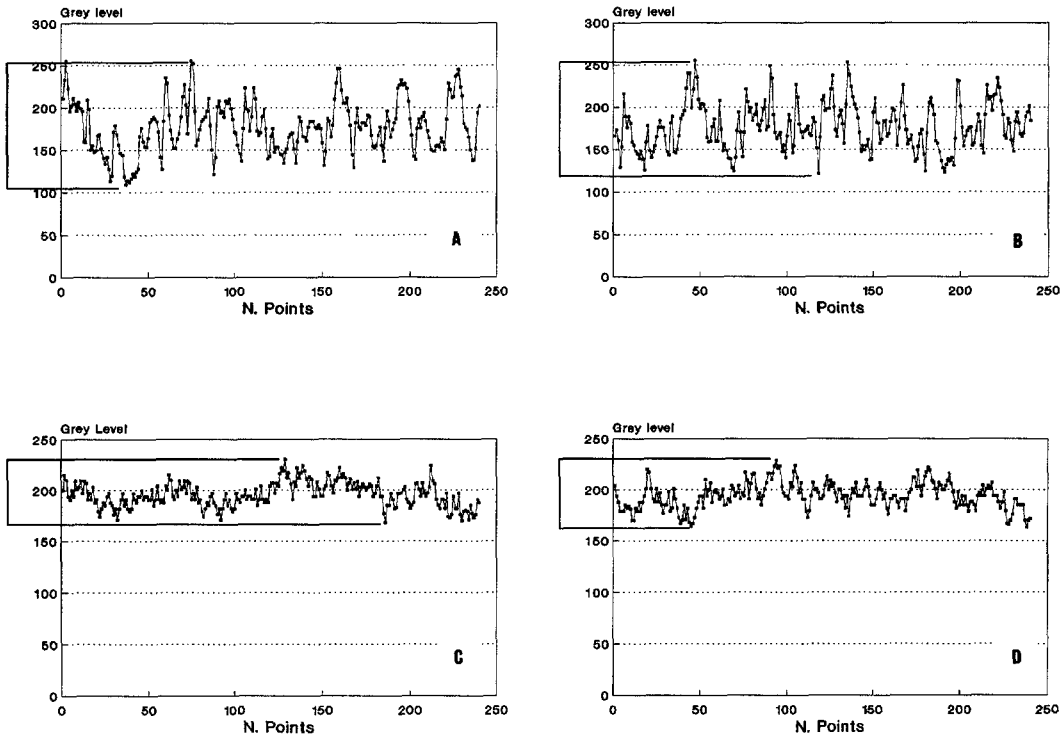

FIG. 3. A–D) Graphics showing the grey levels encountered by the lines (N. Points in size) traced in a perpendicular direction to the direction parallel to the body axis. A–B correspond to the image in Figure 2C and C–D corresponds to the image in Figure 2D. The difference between the maximum and minimum values encountered in the corresponding profile is graphed.

with μ_d corresponding to an average of the differences, C_d, A_d, to measures of contrast, and E_d to uniformity.

Results and Discussion

Lateral fields: The objective of analyzing the lateral fields was to detect lines running parallel to the body axis. The lateral field presented great sensitivity in grey levels, which complicated the use of classic edge detectors (2). Results using the Canny filters were not acceptable for resolving the lines in the lateral field because the boundaries were noises. To resolve this problem, the images were preprocessed with directional filters to highlight these features with a directional component and processed again with the Canny filter to emphasize the line boundaries (Fig. 1). After the boundaries were highlighted, a sample of straight lines perpendicular to them was analyzed for the number of intersections ('010' transitions in the corresponding profile) (Table 1). The number of lines detected were four (every two intersections determine one line).

Annules: The presence and coarseness of annules were analyzed with directional filters, and the profiles of the resultant image were analyzed. The transitions of grey levels (in perpendicular direction to the body axis) on the filtered image were determined and the differential patterns between both graphics were established (Fig. 2). Significant samples of profiles of both graphics were taken and the differences between the maximum and minimum values of the profiles were examined (Table 2), resulting in the classification intervals of $I_1 = [130, 174]$ if coarse annules are present and $I_2 = [48, 97]$ if annules are absent (Fig. 3).

Texture: Esophagus and intestine: The presence and relative position of internal structure, T1 (esophageal gland), and T2 (intestine), were analyzed for overlap, T3,

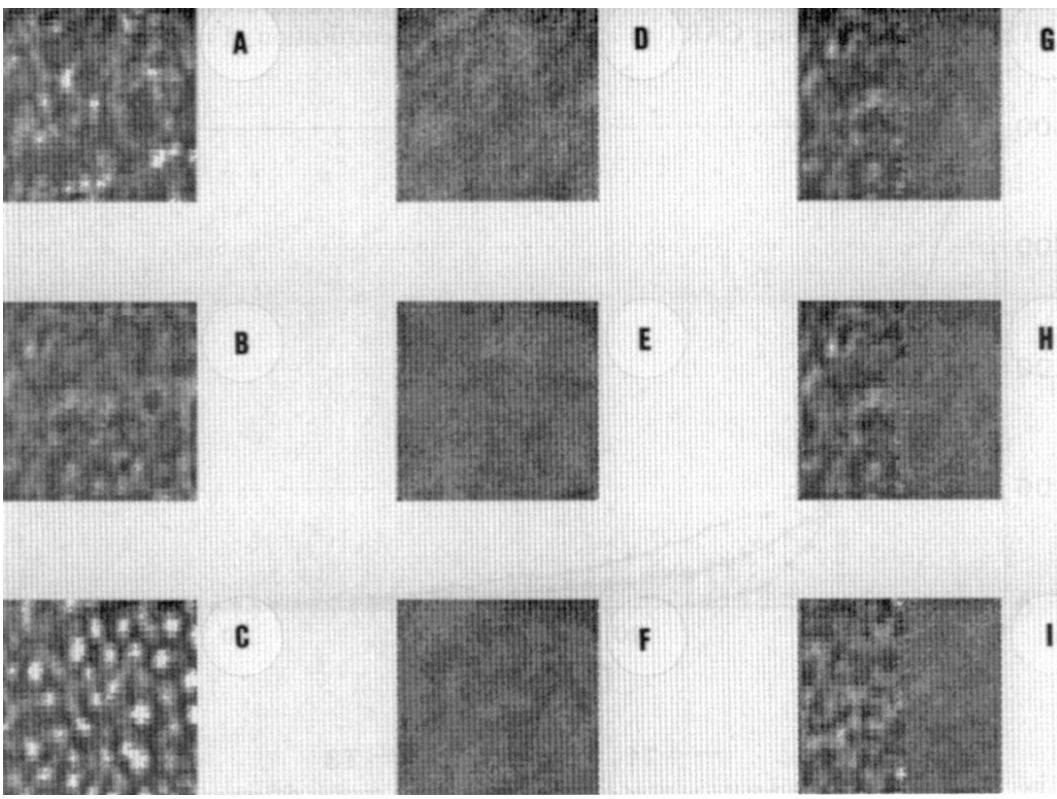

Fig. 4. A–C) Details of textures of esophageal gland (T1). D–F) Details of textures of intestine (T2). G–I) Details of textures of esophageal gland overlapping intestine (T3).

on samples of different species (Fig. 4). A statistical approach (5) was used to classify the textures to discriminate three classes. A vector of the measures was calculated and used with a statistical technique (CART) to determine which of the measures is best for classification. The set of measures used were divided into four categories based on (i) the histogram of grey levels; (ii) differences of grey levels (the number of occurrences of each possible difference of grey level in the image was calculated according to a particular vector of displacement); (iii) occurrences of the same grey level according to a particular vector of displacement; and (iv) co-occurrences of grey levels. The number of times that couples of grey levels occur in a particular spatial relation was determined. In (A) we saw the measures used in point ii.

The vector of measures was constructed subsequently for each texture. An exact and easy-to-interpret rule of prediction was made to isolate the most significant variables for the classification.

The result of applying CART to a matrix of data with 60 rows (20 samples for each texture) and 17 columns (number of selected measures) is shown in a tree (Fig. 6), in which measures x_6 and x_7 are related to the uniformity and the contrast in the differences of grey levels. The behavior of the three examples of textures with respect to the difference of grey levels was illustrated, and showing that T3 is in an intermediate level between T1 and T2 (Fig. 5). In axis x we represent the differences of grey levels in the range [0..255] and in axis y the number of occurrences of each difference in such a way that a value of k for a difference of d indicates that there are k pairs of pixels in the image in a particular spatial relation, which difference of grey level is d.

Image analysis provides tools in nematology for detecting features with a strong directional and textural component. The techniques presented in this paper have been tested on different species of nematodes with very good results. These techniques may in the future make possible automatic identification of nematodes.

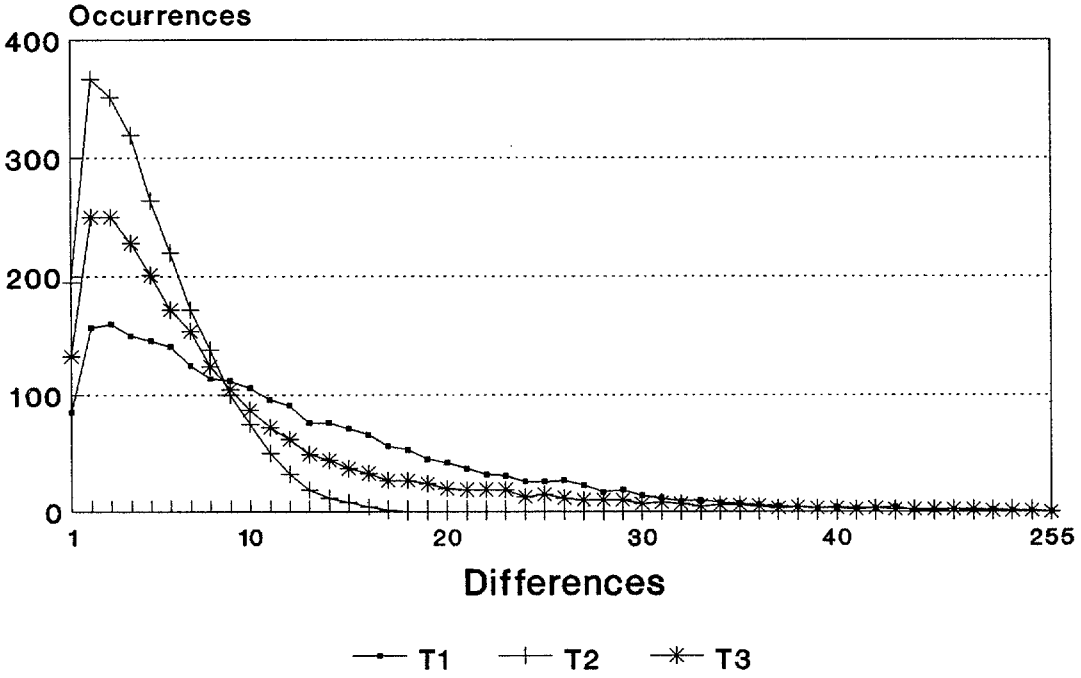

FIG. 5. Graphic representing the number of occurrences of each possible difference of grey level in the three different kinds of textures: T1 (esophageal gland), T2 (intestine), and T3 (esophageal gland overlapping intestine).

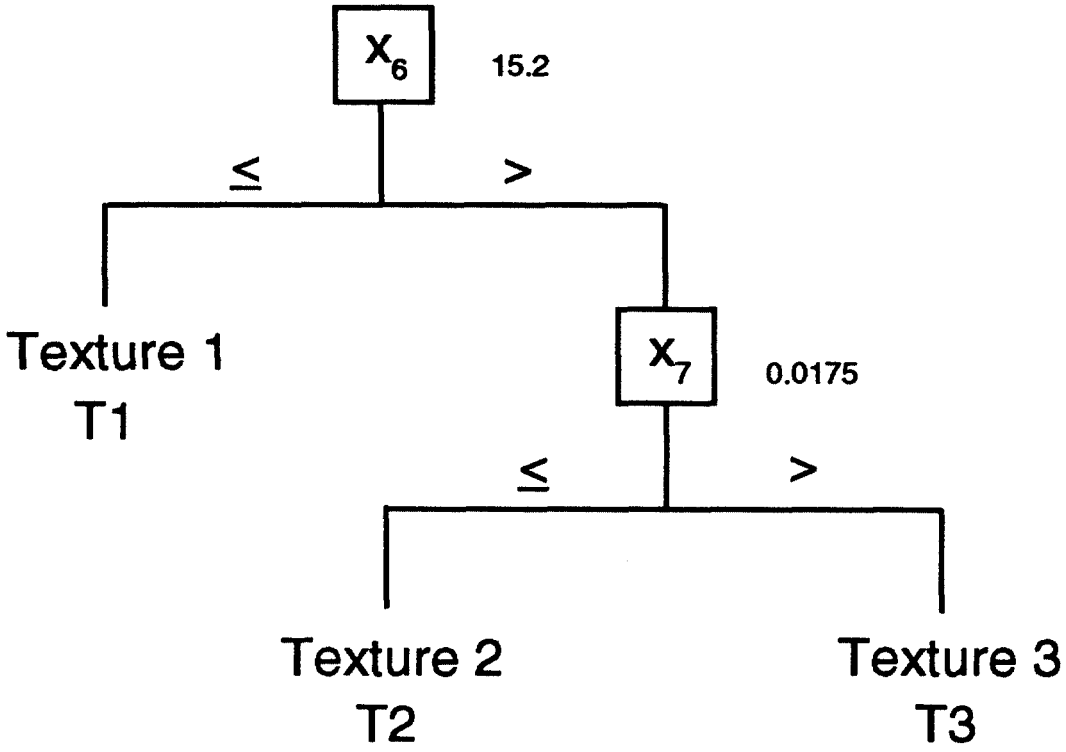

FIG. 6. Classification tree constructed using CART software from three samples of 20 textures each: T1 (esophageal gland), T2 (intestine), and T3 (Esophagus overlapping). Each sample item is represented by a vector of 17 measures. Measures used in the classification were x_6 and x_7, related to the difference of grey levels.

LITERATURE CITED

1. Breiman, L., J. H. Friedman, R. A. Olshen, and C. Stone. 1984. Classification and regression trees. Monterey, CA: Wadsworth.

2. Canny, J. 1986. A computational approach to edge detection. IEEE Transactions on PAMI 6:679–699.

3. De Grisse, A. T. 1969. Redescription ou modifications de quelques techniques utilisées dans l'étude des nématodes phytoparasitaires. Mededelingen fakulteit landbouwwetenschappen Gent 34:351–369.

4. Gonzalez, R. C., and P. Wintz. 1987. Digital image processing. New York: Addison-Wesley.

5. Haralick, R. M. 1979. Statistical and structural approaches to texture. Proceedings of the IEEE 67: 786–804.

6. Levine, M. D. 1985. Vision in man and machine. New York: Mcgraw-Hill.

7. Pérez de la Blanca, N., J. Fdez-Valdivia, P. Castillo, and A. Gomez-Barcina. 1992. Detecting nematode features from digital images. Journal of Nematology 24:289–297.

8. Rosenfeld, A., and A. C. Kak. 1982. Digital picture processing, 2nd ed. Vols. 1 & 2. Orlando, FL: Academic Press.

9. Seinhorst, J. W. 1959. A rapid method for the transfer of nematodes from fixative to anhydrous glycerin. Nematologica 4:67–69.

10. Seinhorst, J. W. 1962. On the killing, fixation and transferring to glycerin of nematodes. Nematologica 8:29–32.